Conformal Frequency-Diverse Metasurface for Computational AoA Detection

Mohammadreza F. Imani, *Member, IEEE*, and Idban Alamzadeh, *Graduate Student Member, IEEE*

***Abstract*—Detecting the angle of arrival (AoA) of electromagnetic waves is an important function in a variety of applications, such as navigation and wireless communication. In this letter, we propose a conformal metasurface antenna (CMA) for detecting the AoA in the horizontal plane. This structure consists of a conformal waveguide with its upper conductor wall fashioned with metamaterial radiators. The resonance frequencies of the metamaterial radiators are selected randomly over a band of operation. The random distribution of resonance frequencies results in patterns that change with frequency and encode information about the AoA of an incident signal into frequency samples, which can be analyzed to retrieve the incident AoA. Using full-wave simulation, we detail the design and operation of the proposed frequency-diverse CMA. We develop and numerically demonstrate a computational processing technique to estimate the AoA from the cross correlation of the signals at the end of coaxial connectors attached to the CMA. The impact of the number of frequency points, bandwidth, and noise on the performance of the device will be illustrated. The proposed device promises a simple and versatile hardware that can detect the AoA from a single receiver and can find application in wireless communication, surveillance, and navigation systems.**

***Index Terms*—Angle of arrival (AoA), computational imaging, conformal antenna, metamaterial, metasurface.**

I. Introduction

DETECTING angles of arrival (AoAs) of electromagnetic (EM) signals is a priority for many civil and military applications. In wireless communication, the information about the AoA is vital to adaptive beamforming and mitigating undesired signal wastage and interference [1], [2], [3]. In tracking devices such as radars, the AoA is continuously tracked to determine the direction of targets [4], [5], [6]. Similarly, autonomous, marine, and aerial vehicles are equipped with direction-finding devices for navigation and/or surveillance [7], [8], [9]. Furthermore, direction-finding mechanisms can also be leveraged in microwave and synthetic aperture radar imaging systems to determine signal scattering characteristics from different directions [10].

Over the years, a plethora of works have been dedicated to the design of antenna hardware or processing algorithm to deduce the AoA from planar structures [11]. However, the AoA detection mechanism can better serve many practical purposes when it can conform to the surface of readily available objects, such as robots, cars, aerial vehicles, missiles, etc. As a result, using conformal antennas and arrays for AoA detection has also gained traction [12], [13], [14]. Array elements on a conformal surface need to be closely spaced to avoid phase ambiguity. As an alternative approach, one can utilize high-gain array elements to mitigate phase ambiguity and improve detection over a wider bandwidth (BW) [15]. The design of conformal antennas for AoA detection, thus, requires navigating a tradeoff between the size of each element (to increase gain) and the spacing of the adjacent elements, which can become complicated especially when there are other restrictions set by the application. Furthermore, almost all the methods above require using many receiving units, which can further complicate the overall cost and complexity. To overcome that issue, some recent works have examined the application of compressive sensing techniques to AoA detection problems [16]. To overcome all these challenges, it is, thus, highly desired to develop a conformal antenna structure that is simple and versatile and allows for the application of compressive AoA detection, where only one or a few receiving units are required.

In the meantime, metasurface antennas have emerged as a simple platform well suited for the application of compressive sensing techniques to microwave imaging problems [17], [18]. This is due to the fact that metasurface antennas, when designed properly, can allow for multiplexing of information, a property that can be leveraged to implement compressive sensing techniques. A simple example of such a metasurface antenna is a waveguide or a cavity with one of its conductive walls patterned with metamaterial radiators with randomly selected resonance frequencies. These metasurfaces could generate frequency-dependent spatially diverse radiation patterns that illuminate the whole region of interest and could multiplex reflectivity maps into fast frequency sweeps. The frequency measurements made in this manner can then be computationally processed to reconstruct the desired image [19]. This concept has been recently applied to AoA detection in planar structures as well [20], [21]. In addition to frequency-diverse metasurface antennas, dynamic metasurface antennas—where each metamaterial radiator is loaded with a switchable component and addressed independently—have also been proposed, and their utility in computational imaging has been established [22]. This concept has also been extended to AoA detection in planar structures [23], [24].

In this letter, we extend the idea of computational AoA detection to conformal metasurface antennas (CMAs). CMAs have been extensively studied for beam steering purposes [25], [26], [27], [28], [29], [30], [31], [32]. However, these works have not explored the application of CMAs to AoA detection. In comparison to conventional conformal antennas and

Manuscript received 7 July 2023; revised 10 August 2023; accepted 12 August 2023. Date of publication 14 September 2023; date of current version 1 November 2023. This work was supported in part by the National Science Foundation award ECCS-2030068 under subaward 333-2727 to Arizona State University.

The authors are with the School of Electrical, Computer, and Energy Engineering, Arizona State University, Tempe, AZ 85287 USA (e-mail: mohammadreza.imani@asu.edu; amuham23@asu.edu).

Digital Object Identifier 10.1109/LAWP.2023.3312041

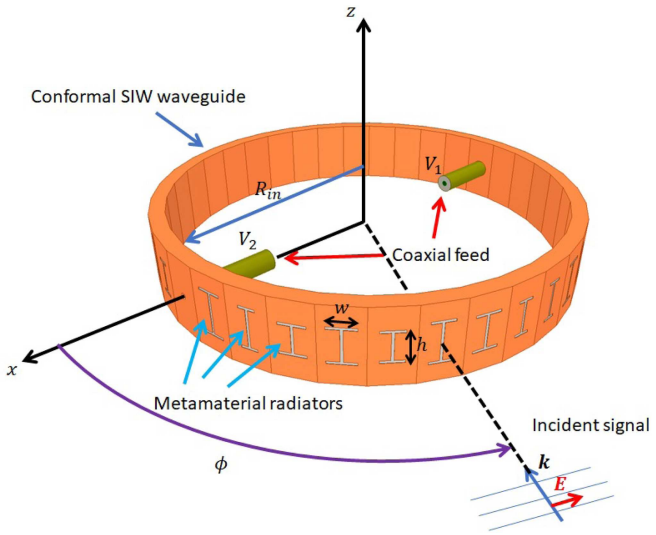

Fig. 1. General configuration of a CMA with frequency-diverse reception patterns.

arrays, CMAs allow for utilizing numerous radiators close to each other on a conformed surface, eliminating the need for high-gain antennas or issues related to phase ambiguity. Since metamaterial radiators are usually subwavelength, they can be implemented easily on any surface of arbitrary curvature. Given these advantages and their utility to implement compressive sensing techniques (to reduce the number of receivers), this letter intends to investigate the application of CMA to AoA detection. Toward this goal, we extend the idea of *information multiplexing* metasurfaces to conformal structures and design a sensing device capable of AoA detection across the entire azimuthal range, i.e., [0–360°]. We will show that the proposed CMA can generate angularly diverse radiation/receiving patterns as a function of frequency. Using these frequency-diverse patterns—which can be characterized using simple cylindrical scans—we can multiplex AoAs of signals into simple frequency measurements at a single port. We then show that the collected frequency reading can be computationally processed to deduce the incident signal's AoA. In addition, we examine the impact of the number of frequency points, BW, and noise on the fidelity of AoA estimation. We conclude this letter by outlining several interesting future directions.

II. Conformal Metasurface Antenna

The proposed device consists of a conformal waveguide exciting a multitude of metamaterial radiators, as shown in Fig. 1. In this letter, we have selected to use substrate integrated waveguides (SIWs) since they have shown great promise in recent works for a successful implementation of conformal antenna geometries [33], [34], [35], [36]. It is worth noting that the proposed operation can be extended to any other waveguide geometry. This SIW is connected to two coaxial connectors on opposite sides. Coaxial feeds are selected for simplicity of their implementation in simulation setup. In a practical implementation, one may excite the SIW via apertures coupled to microstrip lines or from the sides using a coplanar waveguide. Those modifications, however, would not change the main concepts presented in this letter about the feasibility of detecting AoAs using conformal frequency-diverse metasurfaces. For metamaterial radiators, we have selected complementary I-shape resonators [37] due to their simplicity. The resonance frequency of the metamaterial radiators is selected randomly to be within a given band of operation. As the EM signal illuminates this metasurface antenna, it couples to a different set of elements depending on their resonance frequency and location along the array. It is worth noting that owing to the subwavelength size of the metamaterial radiators (and consequently low gain), they can accept signals from almost all the angles in the half-space facing each of them. For example, if a 10 GHz EM wave is illuminating this structure, it can couple to almost all the elements—with resonance frequency near 10 GHz—in the half circle facing that direction. The signal at the end of coaxial connectors would, thus, be a random weighted multiplex version of the incident signal, where the random weights for each frequency will be different. In this manner, we can encode the information about the AoA to frequency measurements at the end of the coaxial connectors.

In this letter, we use the cross correlation of the voltage reading at the end of the coaxial connectors as the measured data. The cross correlation of the two signals can be implemented using analog or digital cross-correlating circuits [38], [39] and is not modeled in this letter for simplicity and brevity. In other words, we plan to use $g = V_1 V_2^* / |V_1 V_2^*|$ as the measurement for each frequency point, where V_1 and V_2 are voltages at the end of the coaxial connectors (see Fig. 1), and * denotes the complex conjugate. Since the information about the incident angle is only present in the phase difference, we will disregard the amplitude of the measured signal.

For demonstration purposes, we select the X-band, i.e., $[8-12]$ GHz, as the frequency band of operation. The SIW is assumed to be made of Rogers/Duroid 5880 with a dielectric constant of 2.2 and a loss tangent of 0.0009. This substrate is selected due to its flexibility and the possibility to conform to arbitrary geometries. To improve the transition from the coaxial connector to the SIW, we selected the thickness of the SIW to be 3.1 mm. For simplicity, we modeled the walls of the SIW with conductive boundary conditions (instead of via walls). The width of the SIW is selected to be 15 mm, which corresponds to a cutoff frequency of 6.742 GHz. In our setup, to simplify the simulation configuration, we assume that the SIW consists of a 36-equal-side regular polyhedron. Each side of the SIW contains one metamaterial radiator. In practical implementation, this design can be fabricated to conform any curvature if needed by bending its flexible substrate. The radius of the SIW polyhedral is $R_{\text{in}} = 45$ mm $= 1.5\lambda$, where $\lambda = 30$ mm is the wavelength at 10 GHz.

The first step in the design of this structure is to find the appropriate combination of length and width for the metamaterial radiators—denoted by h and w in Fig. 1. Toward this goal, we used Ansys HFSS to simulate a single element in a planar SIW of the same cross section as the conformal one, as shown in Fig. 2(a). The transmission between the two ports of this setup is shown in Fig. 2(b) for different combinations of h and w. Using this simulation as the guide, we selected the elements along the SIW randomly to have a width, w, randomly drawn from $[6-9]$ mm, and a height, h, randomly drawn from $[3-5]$ mm. The opening of the I-shape of the metamaterial radiator in all the studies is 0.5 mm.

The CMA designed in this manner is then simulated to analyze its radiation pattern (or reception pattern by reciprocity).

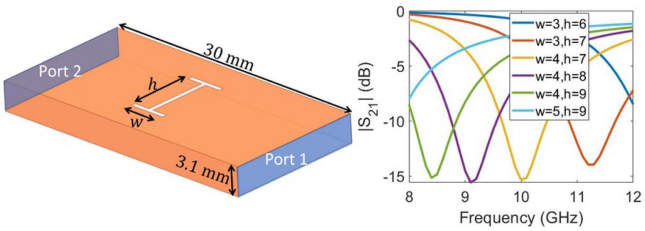

(a) (b)

Fig. 2. (a) Simulation setup for designing metamaterial radiators. (b) Simulated scattering parameter for the setup shown in (a) for different geometrical dimensions of metamaterial element.

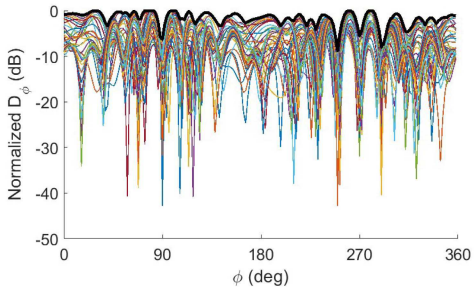

Fig. 3. Normalized radiation patterns of the CMA for 41 frequency points over the X-band. The envelope of the patterns is denoted by the thick black line.

To reduce the simulation complexity and time, we placed the structure between a parallel plate waveguide made of perfect magnetic conducting walls. This way, we can confine our studies to quasi-2-D, where the transmitted/incident electric fields are assumed to be polarized horizontally. The radiation pattern of this structure for the case when both the connectors are excited is shown in Fig. 3. The radiation patterns exhibit clear changes as a function of frequency, thereby verifying the hypothesis that this device has frequency-diverse angularly distinct receiving patterns. Here, we have used 41 frequency points uniformly distributed over the X-band (spacing of 100 MHz). The envelope of the patterns formed at different frequency points is also depicted. We see that, overall, all the angles are received with fairly reasonable strength by this device over the band of operation, i.e., approximating an omnidirectional pattern with angular selectivity.

III. Computational AoA Detection

To utilize the frequency-diverse patterns shown in Fig. 3 for AoA detection, we follow a similar procedure as those in [23] and [24]. The first step is to discretize the range of AoAs (i.e., [0–360°]) into N bins. Next, we simulate the structure in Ansys HFSS with plane waves arriving from the angles at the center of those bins, i.e., ϕ_{ref}. The voltages at the end of the coaxial connectors (terminated in absorbing boundary condition) are computed numerically and correlated with each other. In this manner, we can form an $M \times N$ reference matrix $\mathbf{H}$ for all the N reference angles and M frequency points. The mn entry of this matrix for the mth frequency point, f_m, and the nth reference angle, ϕ^n_{ref}, is, thus, given as

$$h_{mn} = V_1 V_2^* / |V_1 V_2^*| \quad \text{for} \quad f_m, \phi^n_{\text{ref}}. \tag{1}$$

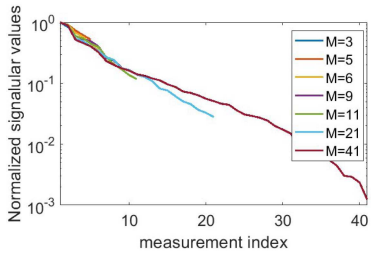

Fig. 4. Normalized singular values for different number of frequency points over the X-band (4 GHz BW).

In practice, one can populate the reference matrix by placing the metasurface on a rotation stage, while a transmitting antenna illuminates it from a distance. It is worth noting that by using the cross correlation of the received signals, the reference matrix becomes independent of the incident signal's phase reference (i.e., the radial distance of the source).

Now, let us consider the case where the incident signal was received from one of the reference directions. In that case, we can write the received signal, $\mathbf{g}$, as

$$\mathbf{g}_{M\times 1} = \mathbf{H}_{M\times N}\mathbf{f}_{N\times 1}. \tag{2}$$

Here, $\mathbf{f}_{N\times 1}$ is a vector whose nth entry is 1 if the incident signal is from the nth reference angle and is zero otherwise. Using $\mathbf{g}$, we can, thus, estimate $\mathbf{f}$ by solving (2). However, $\mathbf{H}$ is not a square matrix, and its inverse is not defined. Furthermore, the incident signal may be from directions other than the reference angle. As a result, we estimate $\mathbf{f}$ by using computational techniques. In this letter, we use the least-squares solver method (implemented as *lsqr* in MATLAB). The result would be a vector $\mathbf{f_{est}}$, which has a peak closest to the actual AoA. We, thus, can estimate any AoA by the reference angle closest to it. In this letter, we select to use $N = 72$ reference angles, separated by 0.0873 rad ($\approx 5°$). Denser discretization of the azimuth plane may be possible but will require a prohibitively lengthy simulation. It is important to note that the resolution of this device, based on a uniform circular array calculation, would be around 13.5°. However, since we are using prior knowledge that a single (predominant) signal is incident on the device, we can detect the AoA with higher resolution, hence, justifying using dense discretization (bin size of 5° instead of 13.5°).

The ability to solve the inverse problem at the heart of the AoA detection [i.e., solving (2)] depends on the number of measurements, M, i.e., frequency points. However, increasing the number of frequency points may not necessarily yield new information since the total number of measurements of a frequency-diverse structure depends on the correlation of frequency samples, which is a function of the number of metamaterial radiators, their quality factor, and the size of the structure (see [40]). Here, we assess the quality of measurements by plotting the singular value decomposition of the sensing matrix, $\mathbf{H}$, for different numbers of frequency points in Fig. 4 (using $N = 72$). We clearly see that increasing the number of frequency points yields a diminishing return. As a compromise between simulation time and measurement diversity, we use frequency points with 100 MHz spacing.

To demonstrate the proposed operation, we have plotted the estimated vector $|\mathbf{f^2_{est}}|$ in Fig. 5(a) for different test angles (selected to be different from reference angles). This figure is

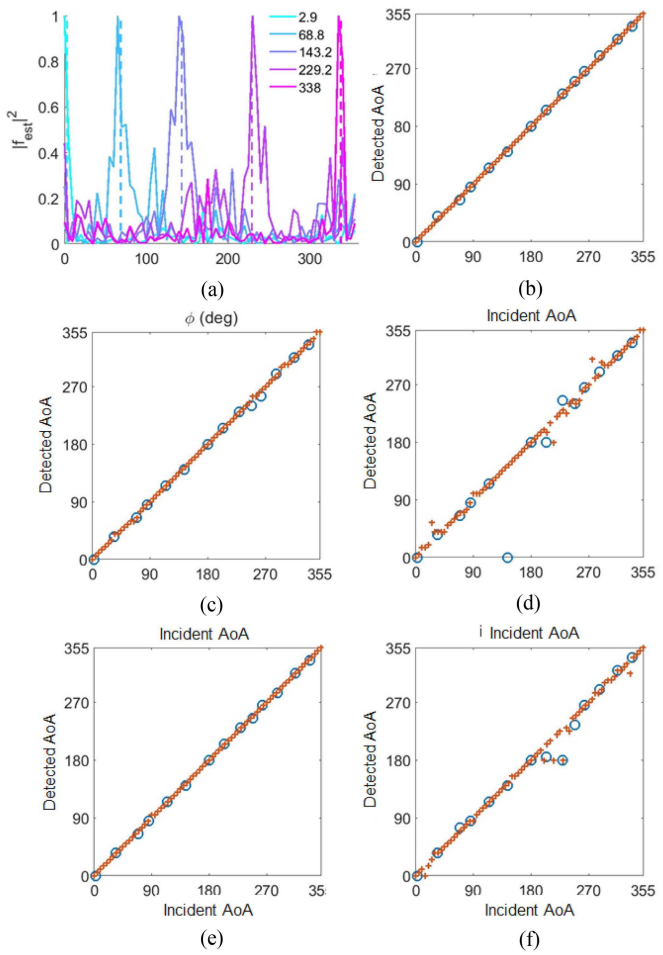

Fig. 5. (a) Reconstructed $|\mathbf{f_{est}}|^2$ for different test angles (dashed lines) at SNR = 50 dB and BW = 4 GHz. Estimated AoA versus incident AoA is plotted in (b) SNR = 50 dB, BW = 4 GHz, (c) SNR = 50 dB, BW = 3 GHz, (d) SNR = 50 dB, BW = 2 GHz, (e) SNR = 20 dB, BW = 4 GHz, and (f) SNR = 10 dB, BW = 4 GHz. In (b)–(e), incident AoA coinciding with ϕ_{ref} is denoted by "+." Otherwise, they are denoted by "○."

obtained at a signal-to-noise ratio (SNR) of 50 dB—noise is assumed to be white Gaussian and is added to V_1 and V_2 using MATLAB built-in additive white Gaussian noise function before calculating $\mathbf{g}$. Examining Fig. 5(a), it is evident that $|\mathbf{f_{est}}^2|$ exhibits a peak at a reference angle closest to the test angle. We have computed the detected AoAs for all the possible tests and reference incident AoAs for SNR of 50 dB. The results are shown in Fig. 5(b). It is important to emphasize that for all the case studies presented in Fig. 5, the sources of incident signal are assumed to be 2 m away from the reference plane used for populating $\mathbf{H}$. The amplitude also fluctuates as a function of frequency (drawn randomly from $[0.5, 1]$). The results in Fig. 5(b) confirm the ability of the proposed device to detect AoAs over the whole horizontal plane even for sources which may not have constant amplitude or are at a different distance from the one used during characterization.

In some applications, it may be desired to use a smaller band of operation. To examine this case, we have reduced the frequency band of operation from 4 GHz in Fig. 5(b) to 3 GHz in Fig. 5(c) and to 2 GHz in Fig. 5(d). It is evident that the proposed method can still operate over a narrower band of operation. However, it requires using more iterations of the least-squares solver to deliver desired performance as the inverse problem becomes more ill-conditioned—since the number of measurements, M, is reduced.

Finally, we examine the impact of noise on the performance of the proposed device. In Fig. 5(e) and (f), we have replotted the cases examined in Fig. 5(b) but with an SNR of 20 and 10 dB, respectively. As the SNR decreases (or the axial distance of the target increases), the spurious peaks shown in Fig. 5(a) can confuse the estimation process. It is evident that the detection of AoA at the SNR of 10 dB becomes slightly less accurate. It is worth noting that the proposed device is examined assuming only one receiving unit. If more receiving units were added to the device (i.e., by adding more connectors), we can improve the performance by increasing the number of measurements and alleviating sensitivity to noise. In fact, using more receivers would also allow for operating with a narrower BW. Alternatively, we can use a low-noise receiver to accommodate low signal levels.

IV. Conclusion and Discussion

In this letter, we designed a conformal frequency-diverse metasurface that can detect the AoA in the horizon using a single receiving unit. The estimation process and operation of the proposed device were detailed. The role of BW, number of frequency points, and noise on the device performance was analyzed. From a practical perspective, this device can be embedded into any shape or configuration. Since it was not designed to form directive beams, its fabrication was not restricted by strict requirements, and any deformation/defect can be accounted for during calibration. Furthermore, this device used a single receiver and only required a frequency sweep, which can be implemented at a low cost. Such a versatile and simple structure for finding the AoA may find application in navigation systems, radars, and wireless communication networks.

This work lays the foundation for applying computational sensing using a CMA. In future works, one can improve the performance by using more elements or by introducing other sources of frequency diversity (such as a planar cavity [20], [21]). Alternatively, one may increase the number of measurements by using more receiving units. Another area to investigate is the estimation process. In this letter, we used simple least-squares solvers. By using more complex compressive sensing techniques or machine learning algorithms [41], [42], we can improve the detection performance. While the dependence on BW is an inherent property of frequency-diverse imaging and sensing systems, it can limit the applications of the device. To remedy this issue, one may implement a conformal dynamic metasurface antenna, where each metamaterial radiator is loaded with a switchable component and addressed independently [32]. It is anticipated that such a structure can detect AoAs using a single frequency of operation [23], [24], [43] and even using only the intensity of the received signal [44]. Demonstrating these exciting possibilities is left for future studies.

References

[1] R. Peng and M. L. Sichitiu, "Angle of arrival localization for wireless sensor networks," in *Proc. 3rd Annu. IEEE Commun. Soc. Sens. Ad Hoc Commun. Netw.*, 2006, pp. 374–382.

[2] M. Li and Y. Lu, "Angle-of-arrival estimation for localization and communication in wireless networks," in *Proc. 16th Eur. Signal Process. Conf.*, 2008, pp. 1–5.

[3] M. Mohanna, M. L. Rabeh, E. M. Zieur, and S. Hekala, "Optimization of music algorithm for angle of arrival estimation in wireless communications," *NRIAG J. Astron. Geophys.*, vol. 2, no. 1, pp. 116–124, 2013.

[4] D. A. Holdsworth, "Angle of arrival estimation for all-sky interferometric meteor radar systems," *Radio Sci.*, vol. 40, no. 06, pp. 1–8, 2005.

[5] J. G. Worms, "Superresolution with conformal broadband antenna arrays," in *Proc. IEEE Radar Conf.*, 2002, pp. 425–431.

[6] F. M. Amjad, A. Z. Sha'ameri, K. M. Yusof, and P. Eberechukwu, "Aircraft position estimation using angle of arrival of received radar signals," *Bull. Elect. Eng. Informat.*, vol. 9, no. 6, pp. 2380–2387, 2020.

[7] A. Berni, "Angle-of-arrival estimation using an adaptive antenna array," *IEEE Trans. Aerosp. Electron. Syst.*, vol. AES-11, no. 2, pp. 278–284, Mar. 1975.

[8] H.-C. Chen, T.-H. Lin, H. Kung, C.-K. Lin, and Y. Gwon, "Determining RF angle of arrival using cots antenna arrays: A field evaluation," in *Proc. IEEE Mil. Commun. Conf.*, 2012, pp. 1–6.

[9] T. Pavlenko, M. Schütz, Y. Dobrev, and M. Vossiek, "Design of sparse dome antenna array for angle of arrival localization systems," in *Proc. 13th Eur. Conf. Antennas Propag.*, 2019, pp. 1–4.

[10] O. Lange and B. Yang, "Antenna geometry optimization for 2D direction-of-arrival estimation for radar imaging," in *Proc. Int. ITG Workshop Smart Antennas*, 2011, pp. 1–8.

[11] E. Tuncer and B. Friedlander, *Classical and Modern Direction-of-Arrival Estimation*. New York, NY, USA: Academic, 2009.

[12] B. Zhang, C. Jin, K. Cao, Q. Lv, and R. Mittra, "Cognitive conformal antenna array exploiting deep reinforcement learning method," *IEEE Trans. Antennas Propag.*, vol. 70, no. 7, pp. 5094–5104, Jul. 2022.

[13] K. Gao, X.-Y. Cao, J. Gao, H.-H. Yang, and J.-F. Han, "Characteristic mode analysis of wideband high-gain and low-profile metasurface antenna," *Chin. Phys. B*, vol. 30, no. 6, 2021, Art. no. 064101.

[14] S. Chengtian, W. Xiaowen, D. Mengqian, and P. Zhihua, "Conformal transmitarray based on metasurface fed by miniaturized filtering antenna," *Microw., Opt. Technol. Lett.*, vol. 65, no. 1, pp. 217–224, 2023.

[15] B. R. Jackson, S. Rajan, B. J. Liao, and S. Wang, "Direction of arrival estimation using directive antennas in uniform circular arrays," *IEEE Trans. Antennas Propag.*, vol. 63, no. 2, pp. 736–747, Feb. 2015.

[16] Q. Shen, W. Liu, W. Cui, and S. Wu, "Underdetermined DOA estimation under the compressive sensing framework: A review," *IEEE Access*, vol. 4, pp. 8865–8878, 2016.

[17] J. Hunt et al., "Metamaterial apertures for computational imaging," *Science*, vol. 339, no. 6117, pp. 310–313, 2013.

[18] M. F. Imani et al., "Review of metasurface antennas for computational microwave imaging," *IEEE Trans. Antennas Propag.*, vol. 68, no. 3, pp. 1860–1875, Mar. 2020.

[19] J. Gollub et al., "Large metasurface aperture for millimeter wave computational imaging at the human-scale," *Sci. Rep.*, vol. 7, no. 1, 2017, Art. no. 42650.

[20] O. Yurduseven, M. A. B. Abbasi, T. Fromenteze, and V. Fusco, "Frequency-diverse computational direction of arrival estimation technique," *Sci. Rep.*, vol. 9, no. 1, 2019, Art. no. 16704.

[21] A. M. Molaei, P. del Hougne, V. Fusco, and O. Yurduseven, "Efficient joint estimation of DOA, range and reflectivity in near-field by using mixed-order statistics and a symmetric MIMO array," *IEEE Trans. Veh. Technol.*, vol. 71, no. 3, pp. 2824–2842, Mar. 2022.

[22] T. Sleasman, M. F. Imani, A. V. Diebold, M. Boyarsky, K. P. Trofatter, and D. R. Smith, "Computational imaging with dynamic metasurfaces: A recipe for simple and low-cost microwave imaging," *IEEE Antennas Propag. Mag.*, vol. 64, no. 4, pp. 123–134, Aug. 2022.

[23] I. Alamzadeh, G. C. Alexandropoulos, N. Shlezinger, and M. F. Imani, "A reconfigurable intelligent surface with integrated sensing capability," *Sci. Rep.*, vol. 11, no. 1, 2021, Art. no. 20737.

[24] I. Alamzadeh and M. F. Imani, "Sensing and reconfigurable reflection of electromagnetic waves from a metasurface with sparse sensing elements," *IEEE Access*, vol. 10, pp. 105954–105965, 2022.

[25] S. Ramalingam, C. A. Balanis, C. R. Birtcher, S. Pandi, and H. N. Shaman, "Axially modulated cylindrical metasurface leaky-wave antennas," *IEEE Antennas Wireless Propag. Lett.*, vol. 17, no. 1, pp. 130–133, Jan. 2018.

[26] Y. Wang, J. Su, Z. Li, Q. Guo, and J. Song, "A prismatic conformal metasurface for radar cross-sectional reduction," *IEEE Antennas Wireless Propag. Lett.*, vol. 19, no. 4, pp. 631–635, Apr. 2020.

[27] R. Ge, R. Striker, and B. Braaten, "A study on conformal metasurface influences on passive beam steering," *Electronics*, vol. 11, no. 5, 2022, Art. no. 674.

[28] D. Rano, A. Yelizarov, A. Skuridin, and E. Zakirova, "Geometric method for determining the phase shift in the reflection of an electromagnetic wave from a conformal meta-surface of a sensing element," *Meas. Techn.*, vol. 65, no. 4, pp. 273–278, 2022.

[29] I. Yoo and D. R. Smith, "Design of conformal array of rectangular waveguide-fed metasurfaces," *IEEE Trans. Antennas Propag.*, vol. 70, no. 7, pp. 6060–6065, Jul. 2022.

[30] J. Wang and R. Yang, "Generating high-purity directive circularly polarized beams from conformal anisotropic holographic metasurfaces," *IEEE Trans. Antennas Propag.*, vol. 70, no. 11, pp. 10718–10723, Nov. 2022.

[31] J. Budhu, L. Szymanski, and A. Grbic, "Design of planar and conformal, passive, lossless metasurfaces that beamform," *IEEE J. Microw.*, vol. 2, no. 3, pp. 401–418, Jul. 2022.

[32] M. R. Hashemi and T. Itoh, "Electronically controlled metamaterial-based leaky-wave transmission-line for conformal surface applications," in *IEEE MTT-S Int. Microw. Symp. Dig.*, 2009, pp. 69–72.

[33] A. J. Martinez-Ros, J. L. Gómez-Tornero, and G. Goussetis, "Conformal tapered substrate integrated waveguide leaky-wave antenna," *IEEE Trans. Antennas Propag.*, vol. 62, no. 12, pp. 5983–5991, Dec. 2014.

[34] K. K. Fan and Z.-C. Hao, "Cylindrical conformal array antenna with tilted H-plane fan-shaped beam for millimeter-wave application," *Microw. Opt. Technol. Lett.*, vol. 58, no. 7, pp. 1666–1671, 2016.

[35] Z.-C. Hao, M. He, and W. Hong, "Design of a millimeter-wave high angle selectivity shaped-beam conformal array antenna using hybrid genetic/space mapping method," *IEEE Antennas Wireless Propag. Lett.*, vol. 15, pp. 1208–1212, 2015.

[36] E. Celenk and N. T. Tokan, "Frequency scanning conformal sensor based on SIW metamaterial antenna," *IEEE Sens. J.*, vol. 21, no. 14, pp. 16015–16023, Jul. 2021.

[37] N. Landy, J. Hunt, and D. R. Smith, "Homogenization analysis of complementary waveguide metamaterials," *Photon. Nanostruct.—Fundam. Appl.*, vol. 11, no. 4, pp. 453–467, 2013.

[38] S. Padin, "A widebandanalog continuum correlator for radio astronomy," *IEEE Trans. Instrum. Meas.*, vol. 43, no. 6, pp. 782–785, Dec. 1994.

[39] C. S. Ruf, "Digital correlators for synthetic aperture interferometric radiometry," *IEEE Trans. Geosci. Remote Sens.*, vol. 33, no. 5, pp. 1222–1229, Sep. 1995.

[40] D. L. Marks, J. Gollub, and D. R. Smith, "Spatially resolving antenna arrays using frequency diversity," *J. Opt. Soc. Amer. A*, vol. 33, no. 5, pp. 899–912, 2016.

[41] C. Wu and J. Elangage, "Multiemitter two-dimensional angle-of-arrival estimator via compressive sensing," *IEEE Trans. Aerosp. Electron. Syst.*, vol. 56, no. 4, pp. 2884–2895, Aug. 2020.

[42] M. Naseri et al., "Machine learning-based angle of arrival estimation for ultra-wide band radios," *IEEE Commun. Lett.*, vol. 26, no. 6, pp. 1273–1277, Jun. 2022.

[43] T. Sleasman, M. Boyarsky, M. F. Imani, T. Fromenteze, J. N. Gollub, and D. R. Smith, "Single-frequency microwave imaging with dynamic metasurface apertures," *J. Opt. Soc. Amer. B*, vol. 34, no. 8, pp. 1713–1726, 2017.

[44] I. Alamzadeh and M. F. Imani, "Detecting angle of arrival on a hybrid RIS using intensity only data," *IEEE Antennas Wireless Propag. Lett.*, early access, 2023, doi: 10.1109/LAWP.2023.3288123.